Proceedings of the Institute of Acoustics & Belgium Acoustical Society
Noise in the Built Environment, Ghent, 29-30 April 2010

EFFECTIVE MEDIUM MODELS FOR GRANULAR MATERIALS AND COMPOSITES

O Umnova University of Salford, Salford, Greater Manchester, UK, M5 4WT
R Venegas University of Salford, Salford, Greater Manchester, UK, M5 4WT
A Krynkin University of Salford, Salford, Greater Manchester, UK, M5 4WT

1 INTRODUCTION

Effective medium models have been used to predict acoustical properties of air saturated granular and fibrous materials for several decades. These models aim to calculate effective dynamic density and dynamic compressibility of the material using the information about its microstructure. It is assumed that the structure can be divided into identical elementary cells. Boundary conditions at the outer boundary of each cell are formulated to account for the presence of the neighbouring particles or fibres. The local distributions of pressure, fluid velocity and temperature inside the cell are calculated. Dynamic density and compressibility are obtained using velocity and temperature values averaged over the cell volume (3D case) or surface (2D case). The outlined procedure can be carried out when the wavelength of sound is larger than size of the particles or fibres.
The aim of this paper is to demonstrate the capabilities of the effective medium modelling by considering two different materials. A model for the acoustical properties of packing of microporous spheres is described in the first part. The packing has two distinctive pore scales, one associated with the intergranular voids (mesoporosity) and another with porosity of the spheres (microporosity). Although a network of very small pores has low permeability and might not be directly accessible for sound, its effect can be substantial in double porosity materials. A hybrid double porosity model presented here is based on the approach described in Ref.[1]. The mesoporosity effects are described using the cell model introduced in Ref.[2]. A model for microporosity is developed which takes into account boundary slip and the adsorption/ desorption effects. Model results are compared with absorption data of granular activated carbon and its limitations are discussed. In the second part the effective medium model for an array of thin elastic shells is presented. It is shown that low frequency shell resonances can be accounted for in dynamic density and compressibility functions of the effective medium. The results are compared with the measurements and numerical solutions**.**

2 EFFECTIVE MEDIUM MODEL FOR GRANULAR MICROPOROUS MATERIALS

2.1 Double porosity model for a packing of spheres

A packing of identical porous spheres is considered, assuming that the wavelength of sound exceeds the size of spheres. Mesoporous structure (i.e. packing of non-porous spheres of the same size as the actual ones) is characterised by porosity ϕ_p, dynamic tortuosity α_p and dynamic compressibility C_p. The microporous structure of the spheres is characterised by porosity ϕ_m, dynamic tortuosity α_m and dynamic compressibility C_m. The overall porosity of the packing is $\phi = \phi_p + (1-\phi_p)\phi_m$.
If high permeability contrast is achieved between mesoporous and microporous domains, then dynamic compressibility of pore fluid in double porosity material can be calculated as [1]:

$$C_{dp} = C_p + (1-\phi_p)F_d(\omega)C_m, \quad (1)$$

where $F_d(\omega)$ is the ratio of the averaged pressure in the microporous domain to the pressure in mesopores.
Assume homogeneous structure of the spherical particle and that inside it sound can only propagate normally to its surface. In this case coefficient $F_d(\omega)$ can be related to a normalized surface impedance Z_{surf} of the sphere:

$$F_d(\omega) = \frac{3}{i\omega a \phi_p} \frac{\rho_0 c^2}{Z_{surf} C_m(\omega)}, \tag{2}$$

where *a* is particle radius. Surface impedance of a porous sphere can be calculated as

$$Z_{surf} = -i \frac{Z_m}{\phi_m \left(\frac{1}{k_m a} - \cot(k_m a) \right)}, \tag{3}$$

which gives

$$F_d(\omega) = \frac{3\phi_m}{\phi_p k_m a} \left(\frac{1}{k_m a} - \cot(k_m a) \right), \tag{4}$$

where $Z_m = \frac{\rho_0 c}{\phi_m} \sqrt{\frac{\alpha_m(\omega)}{C_m(\omega)}}$ and $k_m = \frac{\omega}{c} \sqrt{\alpha_m(\omega) C_m(\omega)}$ are characteristic impedance and the wave number of microporous domain.
The dynamic tortuosity remains equal to $\alpha_p(\omega)$:

$$\alpha_{dp}(\omega) = \alpha_p(\omega). \tag{5}$$

Both $\alpha_p(\omega)$ and $C_p(\omega)$ can be calculated using cell model described in [2]. In the following the "pressure approach" is adopted which assumes that the shear stress vanishes at the boundary of the elementary cell and the stress vector matches the pressure in the effective Darcy medium. The geometry of the cell is shown in Figure 1.To complete the model dynamic density and dynamic compressibility of pore fluid in the microdomain have to be calculated.

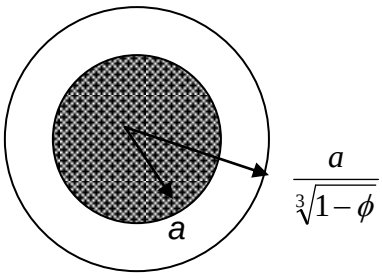

Figure1 Elementary cell, spherical microporous particle

2.2 Microporous domain – effect of boundary slip

Until recently, the validity of zero velocity and fixed temperature boundary conditions on the pore or inclusion surface was assumed in most models of porous sound absorbents. These conditions, however, are violated, if a characteristic pore or inclusion size *R* becomes comparable to a saturating gas molecular mean free path l_{mean}. Their ratio is described by a parameter called Knudsen number, $K = \frac{l_{mean}}{R}$. The continuum description of a gas gives physically justified results when $K \le 0.1$, which imposes a lower limit on the pore or inclusion size, e.g. $R \ge 10 l_{mean}$. For materials saturated by air at normal conditions, this means $R \ge 0.6 \mu m$. However, comparisons with both measurements and molecular dynamics simulations[3] show that continuum approach still provides a satisfactory approximation even Knudsen numbers as high as one.

It is assumed that the pore size of the microporous domain can be comparable to l_{mean}. The influence of the slip effects on the properties of materials with straight pores with different cross section shapes has been studied before[4-5]. However, the assumption of straight pores would present an oversimplification of the porous particle structure. In the following a network of cylindrical fibres is considered. For the sake of completeness, two different fibre orientations are allowed: parallel and perpendicular to the sound propagation direction. According to homogenization theory [1] the air can be considered incompressible at the pore/ inclusion scale. Its motion around an infinitely long cylindrical fibre of radius *R* under a constant pressure gradient $\frac{\partial P}{\partial x} e^{-i\omega t} \mathbf{e_x}$ is described by the following equations:

$$-i\omega\rho_0 \mathbf{u} = -\frac{1}{a}\mathbf{grad}p + \frac{\eta}{R^2}\Delta\mathbf{u} - \frac{\partial P}{\partial x}\mathbf{e_x}, \qquad (6)$$

$$div\mathbf{u} = 0,$$

where $\mathbf{u}$ and p are velocity and pressure, η and ρ_0 are air viscosity and density. All spatial coordinates are normalized by the fibre radius *R*.

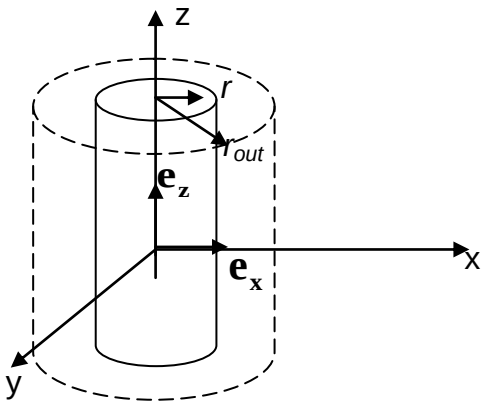

Figure 2 Elementary cell, cylindrical fibre

According to cell model approach the influence of the neighbouring cylinders on the flow can be taken into account assuming that each cylinder is placed at the centre of an imaginary cylindrical cell with radius $r_{out} = \frac{1}{\sqrt{1-\phi_m}}$, where ϕ_m is porosity as before. The geometry of the cell is shown in Figure 2. Boundary conditions of zero normal velocity is assumed at the surface of the fibre, e.g. $u_r(r=1) = 0$. The tangential component of the velocity vector obeys the Maxwell boundary condition: $u_\theta(r=1) = \frac{l_{mean}}{\eta}\tau_{r\theta}(r=1)$, where $\tau_{r\theta}$ is the stress tensor component. It is also assumed that the pressure drop over the cell is equal to the macroscopic pressure gradient, which requires: $p\left(r = \frac{1}{\sqrt{1-\phi_m}}\right) = 0$. The vorticity of the particle velocity is taken to be zero at the outer

cell boundary: $curl\mathbf{u}\left(r=\frac{1}{\sqrt{1-\phi_m}} \right)=0.$ The limitations of the latter assumption as well as the detailed derivations can be found in Ref.[6].

Dynamic tortuosity is derived as the ratio of the macroscopic pressure gradient to the resulting averaged force per unit volume of the fluid $-i\omega\rho_0\langle u_x\rangle$. Assuming that all the fluid is contained within the cells, the averaging can be performed over the surface of a single cell. The calculations result in the following expressions where dynamic tortuosities are presented as functions of angular frequency and Knudsen number:

$$\alpha_{m,\perp}(\omega,K)=(2-\phi_m)-\frac{4(1-\phi_m)}{Q(\kappa)+2(1-\phi_m)+\frac{K\kappa^2}{(1+2K)}\phi_m}, \tag{7}$$

$$\alpha_{m,||}(\omega,K)=1-\frac{2(1-\phi_m)}{Q(\kappa)\phi_m+2(1-\phi_m)+K\kappa^2\phi_m}. \tag{8}$$

Here subscripts $\perp$ and $||$ denote two different sound propagation directions, $\kappa=R\sqrt{\frac{i\omega\rho_0}{\eta}}$,

$$Q(\kappa)=\kappa\frac{H_0^{(1)}(\kappa)J_1\left(\frac{\kappa}{\sqrt{1-\phi_m}}\right)-H_1^{(1)}\left(\frac{\kappa}{\sqrt{1-\phi_m}}\right)J_0(\kappa)}{H_1^{(1)}(\kappa)J_1\left(\frac{\kappa}{\sqrt{1-\phi_m}}\right)-H_1^{(1)}\left(\frac{\kappa}{\sqrt{1-\phi_m}}\right)J_1(\kappa)}.$$

To calculate dynamic compressibility, the following equation for the distribution of temperature $T(r)$ around the fibre subject to an oscillatory pressure $Pe^{-i\omega t}$ has to be solved:

$$N_{pr}\kappa^2T+T''+\frac{1}{r}T'=\frac{N_{pr}\kappa^2}{\rho_0c_p}P, \tag{9}$$

combined with the thermal slip boundary condition at the fibre surface $T(r=1)=\frac{2\gamma K}{(\gamma+1)N_{pr}}T'(r=1)$ and the zero temperature flux condition at the outer cell boundary $T'\left(r=\frac{1}{\sqrt{1-\phi_m}}\right)=0.$ Here c_p is heat capacity under constant pressure, N_{pr} is Prandtl number and γ is adiabatic constant. The normalized dynamic compressibility is defined as $C=\gamma-(\gamma-1)\frac{\rho_0c_p\langle T\rangle}{P}.$ The relationship between dynamic compressibility and dynamic tortuosity $\alpha_{m,||}$ can be easily derived:

$$C_m(\omega,K)=\gamma-\frac{\gamma-1}{\alpha_{m,||}\left(\omega N_{pr},K\frac{2\gamma}{N_{pr}(\gamma+1)}\right)}. \tag{10}$$

Dynamic compressibility does not depend on sound propagation direction.

Expressions for flow resistivity can be derived taking low frequency limit of the dynamic tortuosity functions[7]:

$$\sigma_{m,\perp}(K)=\frac{\sigma_{m,\perp}(K=0)}{1+\frac{4K}{1+2K}F(\phi_m)},$$
$$\sigma_{m,||}(K)=\frac{\sigma_{m,||}(K=0)}{1+4KF(\phi_m)}, \quad (11)$$

where $F(\phi_m)=\frac{\phi_m{}^2}{-2\ln(1-\phi_m)-2\phi_m-\phi_m{}^2}$,

$\sigma_{m,||}(K=0)=0.5\sigma_{m,\perp}(K=0)=\frac{8(1-\phi_m)\eta}{(-2\ln(1-\phi_m)-2\phi_m-\phi_m{}^2)R^2}$. Boundary slip leads to a decrease in flow resistivity values. The effect is stronger for higher porosity and for sound propagating parallel to fibre axes. It can be shown[6] that thermal permeability increases with the Knudsen number while high frequency tortuosity and characteristic viscous and thermal lengths do not change. In fact, for the majority of frequencies, except for the exotically high ones, viscous regime is realized in small pores. This means that the acoustical properties of the microporous network are completely defined by its porosity, tortuosity, flow resistivity and thermal permeability.

2.3 Effect of adsorption

Adsorption and desorption of gas molecules happen at any solid / gas interface. In the presence of sound the adsorption/ desorption equilibrium is violated: extra amount of molecules are adsorbed during the compression phase of the cycle and are released during the rarefaction phase. When the pores are small and tortuous, the inner surface area of the material is large, which makes adsorption effects more noticeable. In this section a semi-empirical model is presented which account for the adsorption in a microporous material [8, 9]. Assume that *n* is the number of the adsorbed moles of gas per unit surface area. The adsorption dynamic equation is

$$\frac{dn}{dt}=k_aP(N-n)-k_dn, \quad (12)$$

where *P* is pressure, *N* is the maximum number of adsorbed moles per unit surface area, k_a and k_d are adsorption and desorption constants. At equilibrium, this equation reduces to the Langmuir's isotherm $n_e=\frac{k_aP_0N}{k_aP_0+k_d}$, where P_0 is atmospheric pressure and n_e is the number of adsorbed molecules at equilibrium.

Assuming small pressure variations in an acoustic wave, $p<<P_0$, equation (12) can be linearised as follows:

$$-i\omega\Delta n=-\frac{1}{\tau}\Delta n+k_ak_dN\tau p, \quad (13)$$

where $\Delta n=n-n_e$, $\tau=\frac{1}{k_aP_0+k_d}$.

This equation should be combined with momentum conservation equation for the gas in pores

$$-i\omega\rho_0\alpha_{dp}(\omega)v=-\frac{\partial p}{\partial x}, \quad (14)$$

and continuity equation

$$-i\omega C_{dp}(\omega)p=-\rho_0c^2\frac{\partial v}{\partial x}+i\omega c^2\mu\Delta n, \quad (15)$$

where $\mu = \frac{P_0}{N_0} c^2$, N_0 is the number of free gas moles.

Now it can be shown that the presence of adsorption lead to changes in dynamic compressibility of air in double porosity material

$$C_{a,dp}(\omega) = C_{dp}(\omega) + \frac{k_a k_d \gamma P_0}{(k_a + k_d P_0)^2} \frac{N}{N_0} \frac{1}{1 - i\omega\tau}. \quad (16)$$

This is in agreement with results obtained in Ref. [9] for cylindrical pores.

2.4 Comparisons with data

For comparisons with the model a sample of granular activated carbon has been chosen. Its properties are summarised in Table 1.

Parameter	**Value**	**Method of determination**
Grain size (mm)	0.425-1.7	measured
Bulk density (g/cm^3)	0.5692	measured
Micropore (less then 2nm) volume (cm^3/g)	0.346	measured
Average grain radius (mm)	0.53	calculated
Porosity ϕ (excluding micropores)	0.634	calculated
Intergranular porosity, ϕ_p	0.34	assumed
Porosity of the grains, ϕ_m	0.45	calculated

Table 1 Properties of the activated carbon sample and methods of their determination.

The particle structure is approximated by an array of fibres perpendicular to sound propagation direction. Despite the irregularities of the particle structure, it was decided to choose $1\mu m$ as an average fibre radius. Adsorption parameters have been taken the same as in Ref.[9].
Predictions and data for the absorption coefficient of 4cm sample are compared in Figure 3. As can be seen the inclusion of adsorption effects improves an agreement between the model and the measurements.

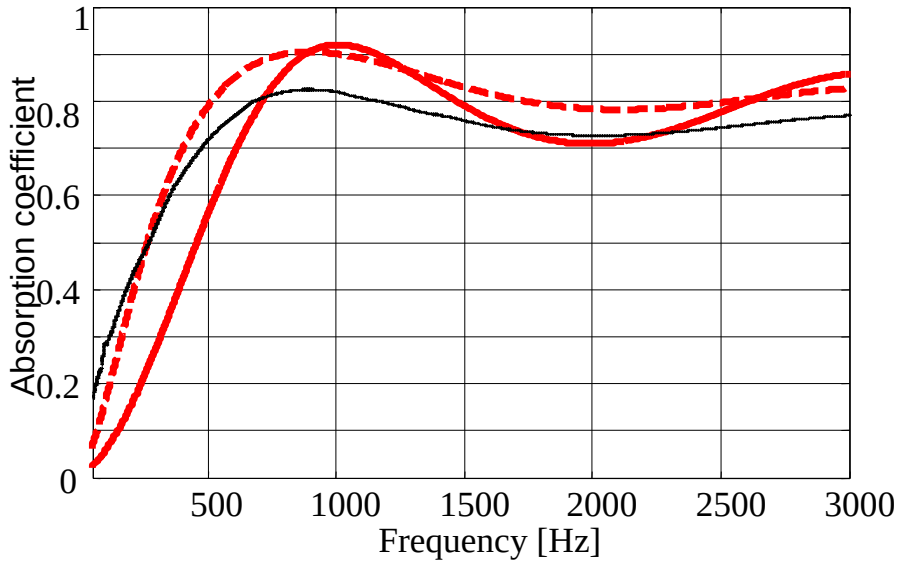

Figure 3 Absorption coefficient. Hard backed layer of activated carbon, thickness 4 cm. Black – data, red solid line – double porosity model, no adsorption, red dashed line – double porosity model with adsorption.

The model however has a limited capability to reflect the real material structure due to 1) idealized geometry, 2) limited amount of information about material parameters.

3 EFFECTIVE MEDIUM MODEL FOR PERIODIC ARRAY OF THIN ELASTIC SHELLS

In Ref.[10] it is shown that in regular array of elastic shells there are at least two low frequency band gaps associated with shell resonances. It is assumed in the following that the shells are much larger than the viscous layer thickness. Due to this viscosity effects in air are neglected. Plane wave is incident normally on the array of identical shells with mid surface radius R and thickness 2*h*, where $\eta = h/R << 1$ Moreover the contrast between the elastic material of the shell and the air is large, e.g. $\varepsilon = \rho_0 c/(\rho c_2) << 1$ and $\varepsilon \sim \eta$. Here ρ and c_2 are density and shear wave velocity of the shell material.

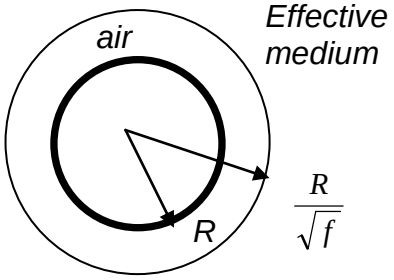

Figure 4 Elementary cell, cylindrical elastic shell

Filling fraction of the array is defined as $f = 1 - \phi$, where ϕ is porosity. The array is divided into elementary cells each consisting of an inclusion surrounded by a layer of air.
The outer radius of the cell is $r_{out} = \frac{R}{\sqrt{f}}$. The medium outside the cell is treated as a homogeneous effective medium (Figure 4). Now the procedure described in Ref.[11] is followed. The acoustic potential in air is

$$P = \sum_{m=-\infty}^{\infty} \left(A_m J_m(k_0 r) + B_m Y_m(k_0 r) \right) e^{im\theta} , \qquad (17)$$

where $k_0 = \frac{\omega}{c}$, *r* is the distance to the centre of the shell, θ is scattering angle. The relationship between coefficients A_m and B_m has been derived in Ref. [10]:

$$S_m = \frac{B_m}{A_m} = \frac{-J'_m(k_0 R)}{Y'_m(k_0 R)}\left[1 + \frac{\hat{U}_{1,m}}{Y'_m(k_0 R)}\right]^{-1}, \quad (18)$$

$$\hat{U}_{1,m} = \frac{\varepsilon}{\pi\kappa_0 R h J'_m(k_0 R)} \frac{m^2 - (k_3 R)^2}{\left(1 + m^2 - (k_3 R)^2\right)}, \quad (19)$$

where $k_3 = \frac{\omega}{c_3}$, c_3 is the dilatational wave speed for a thin elastic plate, $\kappa_0 = c / c_2$, ' stands for derivative with respect to *r*.
In the effective medium the potential is described as

$$P_e = \sum_{m=-\infty}^{\infty}\left(A_m{}^e J_m(k_e r) + B_m{}^e Y_m(k_e r)\right)e^{im\theta}, \quad (20)$$

where $k_e = \frac{\omega}{c}\sqrt{\alpha_e(\omega) C_e(\omega)}$. In this expression $\alpha_e(\omega)$ and $C_e(\omega)$ are unknown dynamic tortuosity and compressibility of the effective medium. Note that in the following the dynamic tortuosity and compressibility are defined as effective quantities of the medium, not its fluid phase as before.
Pressure and normal component of the displacement in air (p and x_r) and in effective medium (p_e and $x_{r,e}$) can be found as

$$p = \rho_0 \omega^2 P \text{ and } x_r = \frac{\partial P}{\partial r}, \quad (21)$$

$$p_e = \rho_0 \alpha_e(\omega) \omega^2 P_e \text{ and } x_{r,e} = \frac{\partial P_e}{\partial r}. \quad (22)$$

At the interface R_{out} between the air and the effective medium the continuity conditions for pressure and normal component of the displacement are applied:

$$\sum_{m=-\infty}^{\infty}\left(A_m J_m(k_0 R_{out}) + B_m Y_m(k_0 R_{out})\right)e^{im\theta} = \alpha_e(\omega)\sum_{m=-\infty}^{\infty}\left(A_m{}^e J_m(k_e R_{out}) + B_m{}^e Y_m(k_e R_{out})\right)e^{im\theta}, \quad (23)$$

$$\sum_{m=-\infty}^{\infty}\left(A_m J'_m(k_0 R_{out}) + B_m Y'_m(k_0 R_{out})\right)e^{im\theta} = \sum_{m=-\infty}^{\infty}\left(A_m{}^e J'_m(k_e R_{out}) + B_m{}^e Y'_m(k_e R_{out})\right)e^{im\theta}. \quad (24)$$

At lower frequencies the scattering is dominated by $m = 0$ and $m = \pm 1$ terms only[11]. According to coherent potential approximation[12], the lowest orders of scattering coefficients in the effective medium have to be zero:

$$B_0{}^e = 0, \; B_{\pm 1}{}^e = 0. \quad (25)$$

Combining these conditions with equations (23)-(24) and retaining the terms to the orders of $(k_0 R_{out})^2$ and $(k_e R_{out})^2$ in the expansions of Bessel functions and their derivatives, the following expressions for $\alpha_e(\omega)$ and $C_e(\omega)$ can be obtained:

$$\alpha_e(\omega)=\frac{1-\dfrac{2f}{\pi(k_0R)^2}S_1}{1+\dfrac{2f}{\pi(k_0R)^2}S_1} \text{ and } C_e(\omega)=1-\frac{4f}{\pi(k_0R)^2}S_0 .$$

Expanding Bessel function derivatives in the expressions for S_0 and S_1 the following equations for the dynamic tortuosity and dynamic compressibility of the effective medium are derived:

$$\alpha_e(\omega)=\frac{2(1+f)-s_1-\left(\dfrac{\omega R}{c_3}\right)^2(1+f-s_1)}{2(1-f)-s_1-\left(\dfrac{\omega R}{c_3}\right)^2(1-f+s_1)}, \quad (26)$$

$$C_e(\omega)=\frac{1-f+s_0-\left(\dfrac{\omega R}{c_3}\right)^2(1-f)}{1+s_0-\left(\dfrac{\omega R}{c_3}\right)^2}, \quad (27)$$

where $s_1=\dfrac{\varepsilon}{2\kappa_0\eta}$ and $s_0=\dfrac{\varepsilon c^2}{\kappa_0\eta c_3{}^2}$.

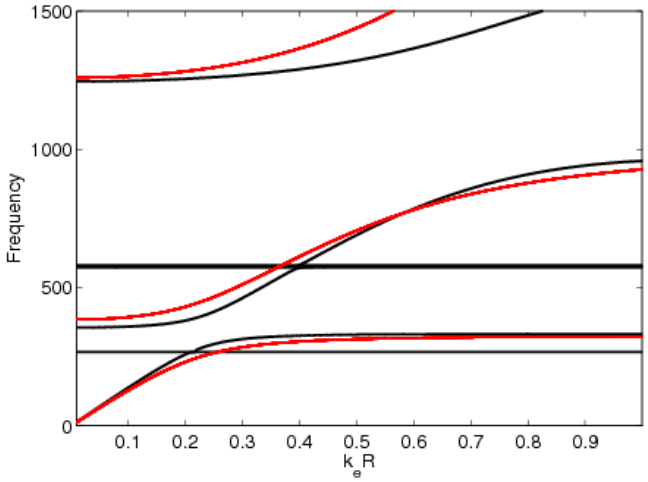

Figure 5 Dispertion relation for the array of elastic shells. Red – effective medium model, Black – exact solution

For the comparisons with the measurements reported in Ref.[10], the following parameters of the shell material and the array are used: *R*=0.0275m, *2h*=0.00025m, *f*=0.37, $c_2=22m/s$, $\rho=1100kg/m^3$, $c_3=46m/s$. With these parameters, equations (26)-(27) predict singularity of the dynamic tortuosity function at 344Hz, while dynamic compressibility becomes singular at 1kHz. Dispersion curves obtained using equations (26)-(27) are compared with the exact solution[10] in Figure 5. Two frequency bands with purely imaginary k_e can be identified. Within these bands the medium does not support any propagating modes. For finite size arrays they correspond to insertion loss (IL) peaks. Transmission measurements on 7X3 array of elastic shells have shown two IL peaks roughly around 400Hz and 1kHz in agreement with effective medium model.

4 CONCLUSIONS

Two variations of the effective medium approach have been used to model the acoustical properties of packing of microporous spheres and the array of resonating elastic shells. It has been shown that boundary slip and adsorption can be taken into account in the framework of the model.
Comparisons with measurements show that effective medium model can adequately describe the main features of the materials behaviour – an increase in low frequency attenuation in the first case and the existence of low frequency band gaps in the second.

5 ACKNOWLEDGEMENT

Part of this work has been supported by the EPSRC research grant EP/E063136/1

6 REFERENCES

1. X.Olny, C.Boutin “Acoustic wave propagation in double porosity media”, J.Acoust.Soc.Am. 114 (1), 73-89 (2003).
2. C. Boutin, C.Geindreau “Estimates and bounds of dynamic permeability of granular media”, J.Acoust.Soc.Am. 124 (6), 3576-3592 (2008).
3. N.G.Hadjiconstantinou, O.Simek, “Sound propagation at small scales under continuum and non-continuum transport”, J.Fluid.Mech. 488, 399-408 (2003).
4. V.F.Kozlov, A.V.Fedorov, N.D.Malmuth, “Acousticl properties of rarefied gasses inside pores of simple geometries”, J.Acoust.Soc.Am. 117, 3402-3411 (2005).
5. M.G.Markov, “Effect of the interfacial slip on the kinematic and dynamic parameters of elastic waves in a fluid-saturated porous medium” Acoust.Phys. 53, 213-216 (2007).
6. O.Umnova, D.Tsiklauri, R. Venegas “Effect of boundary slip on the acoustical properties of microfibrous materials” J.Acoust.Soc.Am. 126, 1850-1861 (2009).
7. D.L. Johnson, J.Koplik, R.Dashen “Theory of dynamic permeability and tortuosity in fluid saturated porous media”, J.Fluid.Mech. 176, 379-402 (1987).
8. F. Bechwati, O.Umnova, T.J.Cox “New semi-empirical model for sound propagation in adsorbing microporous solids (activated carbon)”, in Proceedings of the 19th ICA, Madrid, Spain, 2007.
9. T.Mellow, O.Umnova, K.Drossos, K.Holland, A.Flewitt, L.Karkkainen “On the adsorption-desorption relaxation time of carbon in very narrow ducts” in Proceedings of Acoustics’08 Paris, France (2008).
10. Krynkin, A. and Umnova, O., Characteristics of wave propagation through doubly-periodic array of elastic shells, Euronoise Proceedings, Edinburgh, 2009.
11. J.Mei, Z.Liu, W.Wen, P.Sheng “Effective dynamic density of composites”, Phys.Rev.B 76, 134205 (2007).
12. J.G. Berryman “Long wavelength propagation in composite elastic media. I Spherical inclusions”, J.Acoust.Soc.Am. 68, 1809-1819 (1980).